William & Mary
CHARTERED 1693

W&M ScholarWorks

Arts & Sciences Articles

Arts and Sciences

2015

Ab initio Calculation of the np -> d gamma Radiative Capture Process

Silas R. Beane

Emmanuel Chang

Martin J. Savage

Kostas Orginos
William & Mary

Follow this and additional works at: https://scholarworks.wm.edu/aspubs

Recommended Citation

Beane, Silas R.; Chang, Emmanuel; Savage, Martin J.; and Orginos, Kostas, Ab initio Calculation of the np -> d gamma Radiative Capture Process (2015). *Physical Review Letters*, 115(13). 10.1103/PhysRevLett.115.132001

This Article is brought to you for free and open access by the Arts and Sciences at W&M ScholarWorks. It has been accepted for inclusion in Arts & Sciences Articles by an authorized administrator of W&M ScholarWorks. For more information, please contact scholarworks@wm.edu.

Ab initio calculation of the $np \to d\gamma$ radiative capture process

Silas R. Beane,[1] Emmanuel Chang,[2] William Detmold,[3] Kostas Orginos,[4,5]
Assumpta Parreño,[6] Martin J. Savage,[2] and Brian C. Tiburzi[7,8,9]

(NPLQCD Collaboration)

[1]*Department of Physics, University of Washington, Box 351560, Seattle, WA 98195, USA*
[2]*Institute for Nuclear Theory, University of Washington, Seattle, WA 98195-1560, USA*
[3] *Center for Theoretical Physics, Massachusetts Institute of Technology, Cambridge, MA 02139, USA*
[4]*Department of Physics, College of William and Mary, Williamsburg, VA 23187-8795, USA*
[5]*Jefferson Laboratory, 12000 Jefferson Avenue, Newport News, VA 23606, USA*
[6]*Dept. d'Estructura i Constituents de la Matèria. Institut de Ciències del Cosmos (ICC), Universitat de Barcelona, Martí Franquès 1, E08028-Spain*
[7] *Department of Physics, The City College of New York, New York, NY 10031, USA*
[8]*Graduate School and University Center, The City University of New York, New York, NY 10016, USA*
[9]*RIKEN BNL Research Center, Brookhaven National Laboratory, Upton, NY 11973, USA*

(Dated: September 8, 2015)

Lattice QCD calculations of two-nucleon systems are used to isolate the short-distance two-body electromagnetic contributions to the radiative capture process $np \to d\gamma$, and the photo-disintegration processes $\gamma^{(*)}d \to np$. In nuclear potential models, such contributions are described by phenomenological meson-exchange currents, while in the present work, they are determined directly from the quark and gluon interactions of QCD. Calculations of neutron-proton energy levels in multiple background magnetic fields are performed at two values of the quark masses, corresponding to pion masses of $m_\pi \sim 450$ and 806 MeV, and are combined with pionless nuclear effective field theory to determine these low-energy inelastic processes. At $m_\pi \sim 806$ MeV, using only lattice QCD inputs, a cross-section $\sigma^{806\ \mathrm{MeV}} \sim 17$ mb is found at an incident neutron speed of $v = 2,200$ m/s. Extrapolating the short-distance contribution to the physical pion mass and combining the result with phenomenological scattering information and one-body couplings, a cross section of $\sigma^{\mathrm{lqcd}}(np \to d\gamma) = 334.9(\,^{+5.2}_{-5.4}\,)$ mb is obtained at the same incident neutron speed, consistent with the experimental value of $\sigma^{\mathrm{expt}}(np \to d\gamma) = 334.2(0.5)$ mb.

PACS numbers: 11.15.Ha, 12.38.Gc, 13.40.Gp

The radiative capture process, $np \to d\gamma$, plays a critical role in big-bang nucleosynthesis (BBN) as it is the starting point for the chain of reactions that form most of the light nuclei in the cosmos. Studies of radiative capture [1–3], and the inverse processes of deuteron electro- and photo-disintegration, $\gamma^{(*)}d \to np$ [4–7], have constrained these cross-sections and have also provided critical insights into the interactions between nucleons and photons. They conclusively show the importance of non-nucleonic degrees of freedom in nuclei, which arise from meson-exchange currents (MECs) in the context of nuclear potential models [8, 9]. Nevertheless, in the energy range relevant for BBN, experimental investigations are challenging [10]. For the analogous weak interactions of multi-nucleon systems, considerably less is known from experiment but these processes are equally important. The weak two-nucleon interactions currently contribute the largest uncertainty in calculations of the rate for proton-proton fusion in the Sun [11–17], and in neutrino-disintegration of the deuteron [18], which is a critical process needed to disentangle solar neutrino oscillations. Given the phenomenological importance of electroweak interactions in light nuclei, direct determinations from the underlying theory of strong interaction, quantum chromodynamics (QCD), are fundamental to future theoretical progress. Such determinations are also of significant phenomenological importance for calibrating long-baseline neutrino experiments and for investigations of double beta decay in nuclei. In this Letter, we take the initial steps towards meeting this challenge and present the first lattice QCD (LQCD) calculations of the $np \to d\gamma$ process. The results are in good agreement with experiment and show that QCD calculations of the less well-determined electroweak processes involving light nuclei are within reach. Similarly, the present calculations open the way for QCD studies of light nuclear matrix elements of scalar [19] (and other) currents relevant for dark matter direct detection experiments and other searches for physics beyond the Standard Model.

The low-energy cross section for $np \to d\gamma$ is conveniently written as a multipole expansion in the electromagnetic (EM) field [20, 21],

$$\sigma(np \to d\gamma) \;=\; \frac{e^2(\gamma_0^2+|\mathbf{p}|^2)^3}{M^4\gamma_0^3|\mathbf{p}|}|\tilde{X}_{M1}|^2 + \dots\,, \qquad (1)$$

where $\tilde{X}_{M1}$ is the $M1$ amplitude, γ_0 is the binding momentum of the deuteron, M is the mass of the nucleon, and $\mathbf{p}$ is the momentum of each incoming nucleon in the center-of-mass frame. The ellipsis denotes the contribution from $E1$ and higher-order multipoles (higher multi-

poles can be included systematically and improve the reliability of the description [22], but are not relevant at the level of precision of the present work). In a pionless effective field theory expansion [23–25], employing dibaryon fields to resum effective range contributions [26, 27], the leading-order (LO) and next-to-leading order (NLO) contributions lead to the $M1$ amplitude [27, 28]

$$\tilde{X}_{M1} = \frac{Z_d}{-\frac{1}{a_1}+\frac{1}{2}r_1|\mathbf{p}|^2-i|\mathbf{p}|} \times\left[\frac{\kappa_1\gamma_0^2}{\gamma_0^2+|\mathbf{p}|^2}\left(\gamma_0-\frac{1}{a_1}+\frac{1}{2}r_1|\mathbf{p}|^2\right)+\frac{\gamma_0^2}{2}l_1\right], \quad (2)$$

where $\kappa_1 = (\kappa_p - \kappa_n)/2$ is the isovector nucleon magnetic moment, $Z_d = 1/\sqrt{1-\gamma_0 r_3}$ is the square-root of the residue of the deuteron propagator at the pole with r_3 the effective range in the ${}^3S_1$ channel, and a_1, r_1 are the scattering length and effective range in the ${}^1S_0$ channel. The quantity $l_1 = \tilde{l}_1 - \sqrt{r_1 r_3}\kappa_1$ encapsulates the short-distance two-nucleon interactions through $\tilde{l}_1$, but also depends on κ_1. It is well established that gauge-invariant EM two-nucleon interactions (and direct photon-pion couplings in pionful effective field theories) [12, 18, 22–24, 29–32] must be included in order to determine radiative capture and breakup cross-sections to a precision of better than $\sim 10\%$.

The only quantity in Eqs. (1) and (2) that is not determined by kinematics, single-nucleon properties or scattering parameters, is l_1. In this work, we use LQCD to calculate this quantity by determining the energies of neutron-proton systems in background magnetic fields. A magnetic field mixes the $I_z = j_z = 0$ np states in the ${}^1S_0$ and ${}^3S_1$–${}^3D_1$ channels, providing sensitivity to the EM interactions. In the general situation, including at the physical point, where the deuteron and dineutron have different energy spectra, the formalism developed in Ref. [28] can be used to extract l_1 from the finite-volume energy levels of this coupled system. The deuteron and dineutron ground states are nearly degenerate at both pion masses used in the present calculation [33], and the two-nucleon sector exhibits an approximate spin-flavor SU(4) symmetry (as predicted by the large-N_c limit of QCD [34]). In this case, it can be shown [28, 35] that the energy difference between the two eigenstates depends upon $\tilde{l}_1$ as

$$\Delta E_{{}^3S_1,{}^1S_0}(\mathbf{B}) = 2\left(\kappa_1+\gamma_0 Z_d^2\tilde{l}_1\right)\frac{e}{M}|\mathbf{B}| + \mathcal{O}(|\mathbf{B}|^2)\,, \quad (3)$$

where $\mathbf{B}$ is the background magnetic field. It is convenient to focus on the combination $\overline{L}_1 = \gamma_0 Z_d^2 \tilde{l}_1$ that characterizes the two-nucleon contributions.

Our LQCD calculations were performed on two ensembles of gauge-field configurations generated with a clover-improved fermion action [36] and a Lüscher-Weisz gauge action [37]. The first ensemble had $N_f = 3$ degenerate light-quark flavors with masses tuned to the physical strange quark mass[1], producing a pion of mass $m_\pi \sim 806$ MeV and used a volume of $L^3 \times T = 32^3 \times 48$. The second ensemble had $N_f = 2+1$ flavors with the same strange quark mass and degenerate up and down quarks with masses corresponding to a pion mass of $m_\pi \sim 450$ MeV and a volume of $L^3 \times T = 32^3 \times 96$. Both ensembles had a gauge coupling of $\beta = 6.1$, corresponding to a lattice spacing of $a \sim 0.11$ fm. The details of tuning the quark masses and setting the lattice spacing are similar to those described by the Hadron Spectrum collaboration in generating the anisotropic clover gauge field configurations [38]. Background EM ($U_Q(1)$) gauge fields giving rise to uniform magnetic fields along the x_3-axis were multiplied onto each QCD gauge field in each ensemble (separately for each quark flavor), and these combined gauge fields were used to calculate up-, down-, and strange-quark propagators, which were then contracted to form the requisite nuclear correlation functions using the techniques of Ref. [39]. Calculations were performed on $\sim 1,000$ gauge-field configurations at the SU(3) point and ~ 650 configurations at the lighter pion mass, each taken at intervals of 10 hybrid Monte-Carlo trajectories. On each configuration, quark propagators were generated from 48 uniformly distributed Gaussian-smeared sources for each magnetic field. For further details of the production at the SU(3)-symmetric point, see Refs. [33, 40, 41] and in particular, Ref. [35]. Analogous methods were employed for the calculations using the lighter pion mass ensemble.

Background EM fields have been used extensively to calculate electromagnetic properties of hadrons, such as the magnetic moments of the lowest-lying baryons [42–50] and light nuclei [41], and the polarizabilities of mesons and baryons [50, 51]. The quark fields have electric charges $Q_u = +2/3$ and $Q_{d,s} = -1/3$ for the up-, down- and strange-quarks, respectively, and background magnetic fields are required to be quantized [52] in order that the magnetic flux is uniform throughout the lattice. The link fields, $U_\mu^{(Q)}(x)$, associated with the background field are of the form

$$U_\mu^{(Q)}(x) = e^{i\frac{6\pi Q_q \tilde{n}}{L^2}x_1\delta_{\mu,2}} \times e^{-i\frac{6\pi Q_q\tilde{n}}{L}x_2\delta_{\mu,1}\delta_{x_1,L-1}}\,, \quad (4)$$

for quark flavor q, where $\tilde{n}$ is an integer. The uniform magnetic field resulting from these links is $e\,\mathbf{B} = 6\pi\tilde{n}/L^2\hat{\mathbf{z}}$, where e is the magnitude of the electric charge and $\hat{\mathbf{z}}$ is a unit vector in the x_3-direction. In physical units, the background magnetic fields used with these ensembles of gauge configurations are $e|\mathbf{B}| \sim 0.05|\tilde{n}|$ GeV^2. To optimize the re-use of light-quark propagators in the

[1] The physical value of m_s is used, with nonlinear mass dependence and discretization effects shifting the pseudoscalar meson mass from the leading order chiral perturbation theory estimate, $m_\pi \sim 680$ MeV.

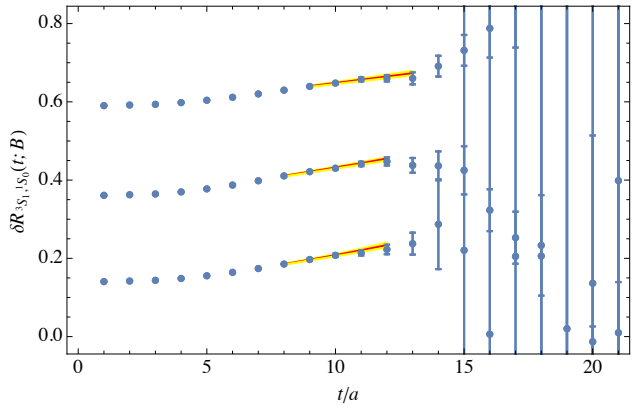

FIG. 1: The double ratios of the two principal correlators are shown for $m_\pi \sim 450$ MeV for the three magnetic field strengths. The bands correspond to the single-exponential fits to the correlator and the associated statistical uncertainty.

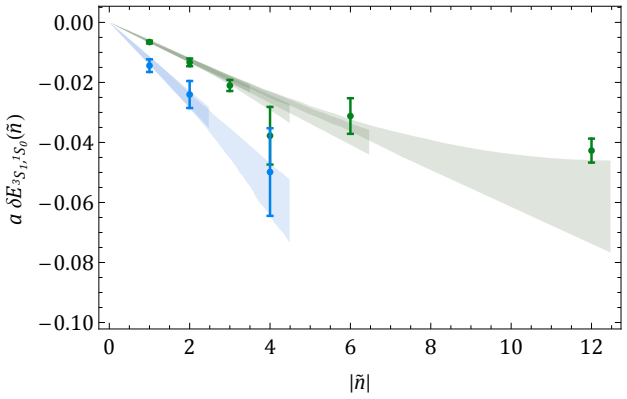

FIG. 2: LQCD calculations of the energy-splittings between the two lowest-lying eigenstates, with the single-nucleon contributions removed, as a function of $\tilde{n}$, along with the associated fits. The lower (blue) set of points correspond to the $m_\pi \sim 450$ MeV ensemble and the upper (green) points to $m_\pi \sim 806$ MeV. The slope of the sets of points is proportional to $\overline{L}_1$ at the appropriate pion mass.

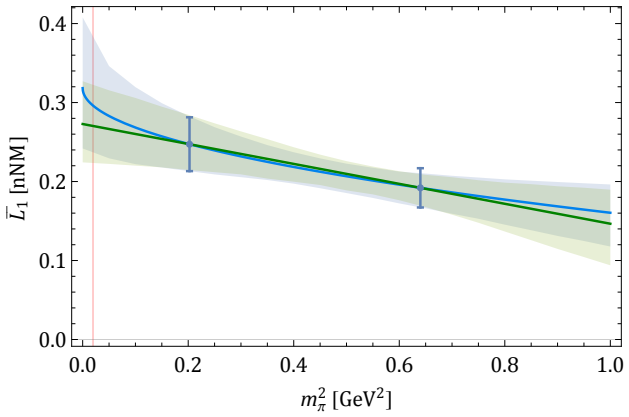

FIG. 3: The results of LQCD calculations of $\overline{L}_1$ (blue points). The blue (green) shaded regions point show the linear (quadratic) in m_π extrapolation of $\overline{L}_1$ to the physical pion mass (dashed line) in natural nuclear magnetons (nNM). The vertical (red) line indicates the physical pion mass.

calculations, $U_Q(1)$ fields with $\tilde{n} = 0, 1, -2, 4$ were used. At the SU(3) symmetric point, additional calculations were performed with $\tilde{n} = 3, -6, 12$.

With three degenerate flavors of light quarks, and a traceless electric-charge matrix, there are no contributions from the magnetic field coupling to sea quarks at the SU(3) point at leading order in the electric charge. This is not the case for the $m_\pi \sim 450$ MeV calculations because of flavor SU(3) breaking. However, $\overline{L}_1$ is an isovector quantity in which sea quark contributions cancel (the up and down sea quarks used in this work are degenerate) so it is correctly determined by the present calculations.

In this work, we focus on the $I_z = j_z = 0$ coupled-channel neutron-proton systems. Our analysis follows that of Ref. [35] which presents results on the $m_\pi \sim$806 MeV ensemble, and we direct the reader to that work for more detail regarding the interpolating operators and statistical analysis methods that are used. A matrix of correlation functions generated from source and sink operators associated with $^3S_1$ and $^1S_0$ $I_z = j_z = 0$ interpolating operators

$$\mathbf{C}(t;\mathbf{B}) \;=\; \begin{pmatrix} C^{^3S_1,^3S_1}(t;\mathbf{B}) & C^{^3S_1,^1S_0}(t;\mathbf{B}) \\ C^{^1S_0,^3S_1}(t;\mathbf{B}) & C^{^1S_0,^1S_0}(t;\mathbf{B}) \end{pmatrix} , \quad (5)$$

is diagonalized to yield "principal correlators", $\lambda_\pm(t;\mathbf{B})$, which exponentially converge to the eigenstates of the coupled system at large times. In all cases, the principal correlators exhibit single-exponential behavior at times where statistical uncertainties are manageable. To highlight the difference arising from purely two-body effects, a ratio of ratios of the principal correlators to the appropriate single particle correlation functions is formed

$$\delta R^{^3S_1,^1S_0}(t;\mathbf{B}) \;=\; \frac{\lambda_+(t;\mathbf{B})}{\lambda_-(t;\mathbf{B})} \frac{C_{n,\uparrow}(t;\mathbf{B}) C_{p,\downarrow}(t;\mathbf{B})}{C_{n,\downarrow}(t;\mathbf{B}) C_{p,\uparrow}(t;\mathbf{B})} , \quad (6)$$

where $C_{p/n,\uparrow/\downarrow}(t;\mathbf{B})$ are the correlation functions corresponding to the different polarizations of the proton and neutron. For large time separations,

$$\delta R^{^3S_1,^1S_0}(t\to\infty;\mathbf{B}) \to A\; e^{-\delta E^{^3S_1,^1S_0}(\mathbf{B}) t} , \quad (7)$$

where A is an overlap factor and the energy shift is

$$\begin{aligned} \delta E^{^3S_1,^1S_0} \;&\equiv\; \Delta E^{^3S_1,^1S_0} - [E_{p,\uparrow} - E_{p,\downarrow}] + [E_{n,\uparrow} - E_{n,\downarrow}] \\ &\to\; 2\overline{L}_1 |e\mathbf{B}|/M + \mathcal{O}(\mathbf{B}^2) , \end{aligned} \quad (8)$$

omitting the $\mathbf{B}$ dependence for clarity. Fig. 1 shows the above ratios for the $m_\pi \sim 450$ MeV ensemble for each magnetic field strength, along with correlated single-exponential fits to the time dependence and their statistical uncertainties. The $\chi^2/d.o.f.$ of these fits are $\mathcal{O}(1)$

in each case. The energies extracted from these fits depend on $|\mathbf{B}|$, with $2\frac{e}{M}\overline{L}_1$ being the coefficient of the linear term. Fig. 2 shows the extracted energy shifts for both the $m_\pi \sim 450$ MeV and 806 MeV ensembles. The figure also shows the envelopes of a large range of polynomial fits to their magnetic field dependence. Uncertainties associated with fit parameters are determined using bootstrap resampling in order to account for the correlations between energy shifts extracted at different magnetic fields from the same configurations. Ref. [35] presents the $m_\pi \sim 806$ MeV correlation functions in detail, and has a complete discussion of the fitting methods used in the analysis for both sets of pion masses.

The extracted values of $\overline{L}_1$ are shown in Fig. 3 for both sets of quark masses. The functional dependence of $\overline{L}_1$ on the light-quark masses is not known. However, the deuteron and dineutron remain relatively near threshold over a large range of quark masses [33, 53–56], and the magnetic moments of the nucleons are essentially independent of the quark masses when expressed in units of natural nuclear magnetons [41], so it is plausible that $\overline{L}_1$ also varies only slowly with the pion mass. Indeed, there is only a small difference in the value of $\overline{L}_1$ at $m_\pi \sim 806$ MeV and at $m_\pi \sim 450$ MeV. In order to connect to the physical point, we extrapolate both linearly and quadratically in the pion mass by resampling the probability distribution functions of $\overline{L}_1$ determined by the field-strength dependence fits at each pion mass. The two forms of extrapolation yield consistent values at the physical point, with the central value and uncertainties determined from the 0.17, 0.50 and 0.83 quantiles of the combination of the two projected probability distribution functions. After this extrapolation, the value $\overline{L}_1^{\rm lqcd} = 0.285(\,^{+63}_{-60}\,)$ nNM is found at the physical pion mass, where the uncertainty incorporates statistical uncertainties, correlator fitting uncertainties, field-strength dependence fitting uncertainties, lattice spacing, and the uncertainties in the mass extrapolation. Using the precise phenomenological values of $\gamma_0 = 45.681$ MeV, $r_1 = 2.73(3)$ fm, $r_3 = 1.749$ fm and $\kappa_1 = 2.35295$ NM, this leads to a value $l_1^{\rm lqcd} = -4.41(\,^{+15}_{-16}\,)$ fm. Future calculations with lighter quark masses will reduce both the statistical and systematic uncertainties associated with $\overline{L}_1$.

The cross section for $np \to d\gamma$ has been precisely measured in experiments at an incident neutron speed of $v = 2,200$ m/s [1]. Using the expressions in Eqs. (1) and (2), the experimentally determined deuteron binding energy and ${}^1S_0$ scattering parameters, the experimentally determined nucleon isovector magnetic moment, and the above extrapolated LQCD value of $l_1^{\rm lqcd}$, leads to a cross section at $v = 2,200$ m/s of

$$\sigma^{\rm lqcd} \;=\; 334.9(\,^{+5.2}_{-5.4}\,)\ {\rm mb} \quad , \tag{9}$$

which is consistent with the experimental value of $\sigma^{\rm expt} = 334.2(0.5)$ mb [1] within uncertainties (see also, Ref. [10]). As in the phenomenological determination, the two-body contributions are $\mathcal{O}(10\%)$. At the quark masses where the lattice calculations are performed, the cross-sections are considerably smaller than at the physical point, primarily because the deuteron binding energy is larger. At $m_\pi \sim 806$ MeV, the scattering parameters, binding energy and magnetic moments have been determined previously [33, 40, 41] and we can predict the scattering cross section using only lattice QCD inputs, with a median value $\sigma^{806\ {\rm MeV}} \sim 17$ mb at $v = 2,200$ m/s.[2]

Summary: Lattice QCD calculations have been used to determine the short-distance two-nucleon interactions with the electromagnetic field (meson-exchange currents in the context of nuclear potential models) that make significant contributions to the low-energy cross-sections for $np \to d\gamma$ and $\gamma^{(*)}d \to np$. This was facilitated by the pionless effective field theory which provides a clean separation of long-distance and short-distance effects along with a concise analytic expression for the near-threshold cross sections. A (naive) extrapolation of the LQCD results to the physical pion mass is in agreement with the experimental determinations of the $np \to d\gamma$ cross-section, within the uncertainties of the calculation and of the experiment. Calculations were performed at a single lattice spacing and volume, introducing systematic uncertainties in $\overline{L}_1$ that are expected to be small in comparison to our other uncertainties, $\mathcal{O}(a^2\Lambda_{\rm QCD}^2, e^{-m_\pi L}, e^{-\gamma_0 L}) \lesssim 4\%$. A more complete study, and a reduction of the uncertainties of this cross-section will require additional calculations at smaller lattice spacings and larger volumes, along with calculations at smaller quark masses.

The present calculation demonstrates the power of lattice QCD methods to address complex processes of importance to nuclear physics directly from the Standard Model. The methods that are used are equally applicable to weak processes such as $pp \to de^+\nu$, $\nu d \to ppe^+$, $\nu d \to \nu d$, and $\nu d \to \nu np$, as well as to higher-body transitions. Background field techniques will also enable the extraction of nuclear matrix elements of other currents relevant for searches for physics beyond the Standard Model. Extensions of our studies to larger systems are currently under consideration, and calculations in background axial-vector fields necessary to address weak interaction processes are under way. As this technique has successfully recovered the short-distance contributions to $np \to d\gamma$, it also seems likely that it can be generalized to the calculation of parity-violating observables in this process resulting from weak interactions, or from physics beyond the Standard Model (see Ref. [57] for a review). Finally, the present work reinforces the utility of combining lattice QCD calculations with low-energy effective

[2] Propagation of the uncertainties in the required inputs leads to a highly non-Gaussian distribution of $\sigma^{806\ {\rm MeV}}$ [35].

field theories describing multi-nucleon systems [58].

We are grateful to Z. Davoudi for discussions and comments. Calculations were performed using computational resources provided by the Extreme Science and Engineering Discovery Environment (XSEDE), which is supported by National Science Foundation grant number OCI-1053575, NERSC (supported by U.S. Department of Energy Grant Number DE-AC02-05CH11231), and by the USQCD collaboration. This research used resources at the Oak Ridge Leadership Computing Facility at the Oak Ridge National Laboratory, which is supported by the Office of Science of the U.S. Department of Energy under Contract No. DE-AC05-00OR22725. Parts of the calculations made use of the `chroma` software suite [59]. SRB was partially supported by NSF continuing grant PHY1206498 and by DOE grant DOE DE-SC0013477. EC was supported by DOE SciDAC grant DE-SC0010337-ER42045. WD was supported by the U.S. Department of Energy Early Career Research Award DE-SC0010495. KO was supported by the U.S. Department of Energy through Grant Number DE- FG02-04ER41302 and through Grant Number DE-AC05-06OR23177 under which JSA operates the Thomas Jefferson National Accelerator Facility. The work of AP was supported by the contract FIS2011-24154 from MEC (Spain) and FEDER. MJS were supported by DOE grant No. DE-FG02-00ER41132. BCT was supported in part by a joint City College of New York-RIKEN/Brookhaven Research Center fellowship, a grant from the Professional Staff Congress of the CUNY, and by the U.S. National Science Foundation, under Grant No. PHY12-05778.

[1] A. Cox, S. Wynchank, and C. Collie, Nuclear Physics **74**, 497 (1965).
[2] A. Tomyo, Y. Nagai, T. Suzuki, T. Kikuchi, T. Shima, T. Kii, and M. Igashira, Nuclear Physics A **718**, 401 (2003).
[3] Y. Nagai, T. Suzuki, T. Kikuchi, T. Shima, T. Kii, et al., Phys.Rev. **C56**, 3173 (1997).
[4] K. Y. Hara, H. Utsunomiya, S. Goko, H. Akimune, T. Yamagata, et al., Phys.Rev. **D68**, 072001 (2003).
[5] R. Moreh, T. Kennett, and W. Prestwich, Phys.Rev. **C39**, 1247 (1989).
[6] E. Schreiber, R. Canon, B. Crowley, C. Howell, J. Kelley, et al., Phys.Rev. **C61**, 061604 (2000).
[7] W. Tornow, N. Czakon, C. Howell, A. Hutcheson, J. Kelley, et al., Phys.Lett. **B574**, 8 (2003), nucl-ex/0309009.
[8] D. Riska and G. Brown, Phys.Lett. **B38**, 193 (1972).
[9] J. Hockert, D. Riska, M. Gari, and A. Huffman, Nucl.Phys. **A217**, 14 (1973).
[10] S. Ando, R. Cyburt, S. Hong, and C. Hyun, Phys.Rev. **C74**, 025809 (2006), nucl-th/0511074.
[11] X. Kong and F. Ravndal, Phys.Rev. **C64**, 044002 (2001), nucl-th/0004038.
[12] M. Butler and J.-W. Chen, Phys.Lett. **B520**, 87 (2001), nucl-th/0101017.
[13] S. Ando, J. Shin, C. Hyun, S. Hong, and K. Kubodera, Phys.Lett. **B668**, 187 (2008), 0801.4330.
[14] E. Adelberger, A. Balantekin, D. Bemmerer, C. Bertulani, J.-W. Chen, et al., Rev.Mod.Phys. **83**, 195 (2011), 1004.2318.
[15] J.-W. Chen, C.-P. Liu, and S.-H. Yu, Phys.Lett. **B720**, 385 (2013), 1209.2552.
[16] L. Marcucci, R. Schiavilla, and M. Viviani, Phys.Rev.Lett. **110**, 192503 (2013), 1303.3124.
[17] G. Rupak and P. Ravi, Phys.Lett. **B741**, 301 (2014), 1411.2436.
[18] M. Butler, J.-W. Chen, and X. Kong, Phys.Rev. **C63**, 035501 (2001), nucl-th/0008032.
[19] S. Beane, S. Cohen, W. Detmold, H. W. Lin, and M. Savage, Phys.Rev. **D89**, 074505 (2014), 1306.6939.
[20] H. Bethe and C. Longmire, Phys.Rev. **77**, 647 (1950).
[21] H. P. Noyes, Nucl.Phys. **74**, 508 (1965).
[22] G. Rupak, Nucl.Phys. **A678**, 405 (2000), nucl-th/9911018.
[23] D. B. Kaplan, M. J. Savage, and M. B. Wise, Phys.Rev. **C59**, 617 (1999), nucl-th/9804032.
[24] D. B. Kaplan, M. J. Savage, and M. B. Wise, Nucl.Phys. **B534**, 329 (1998), nucl-th/9802075.
[25] U. van Kolck, Nucl.Phys. **A645**, 273 (1999), nucl-th/9808007.
[26] D. B. Kaplan, Nucl.Phys. **B494**, 471 (1997), nucl-th/9610052.
[27] S. R. Beane and M. J. Savage, Nucl.Phys. **A694**, 511 (2001), nucl-th/0011067.
[28] W. Detmold and M. J. Savage, Nucl.Phys. **A743**, 170 (2004), hep-lat/0403005.
[29] J.-W. Chen, G. Rupak, and M. J. Savage, Nucl.Phys. **A653**, 386 (1999), nucl-th/9902056.
[30] J.-W. Chen, G. Rupak, and M. J. Savage, Phys.Lett. **B464**, 1 (1999), nucl-th/9905002.
[31] M. Butler and J.-W. Chen, Nucl.Phys. **A675**, 575 (2000), nucl-th/9905059.
[32] M. Butler, J.-W. Chen, and P. Vogel, Phys.Lett. **B549**, 26 (2002), nucl-th/0206026.
[33] S. Beane et al. (NPLQCD), Phys.Rev. **D87**, 034506 (2013), 1206.5219.
[34] D. B. Kaplan and M. J. Savage, Phys.Lett. **B365**, 244 (1996), hep-ph/9509371.
[35] E. Chang, W. Detmold, K. Orginos, A. Parreno, M. J. Savage, B. C. Tiburzi, and S. R. Beane (2015), 1506.05518.
[36] B. Sheikholeslami and R. Wohlert, Nucl.Phys. **B259**, 572 (1985).
[37] M. Lüscher and P. Weisz, Commun.Math.Phys. **97**, 59 (1985).
[38] H.-W. Lin et al. (Hadron Spectrum), Phys. Rev. **D79**, 034502 (2009), 0810.3588.
[39] W. Detmold and K. Orginos, Phys.Rev. **D87**, 114512 (2013), 1207.1452.
[40] S. Beane et al. (NPLQCD), Phys.Rev. **C88**, 024003 (2013), 1301.5790.
[41] S. Beane, E. Chang, S. Cohen, W. Detmold, H. Lin, et al., Phys.Rev.Lett. **113**, 252001 (2014), 1409.3556.
[42] C. W. Bernard, T. Draper, K. Olynyk, and M. Rushton, Phys.Rev.Lett. **49**, 1076 (1982).
[43] G. Martinelli, G. Parisi, R. Petronzio, and F. Rapuano, Phys.Lett. **B116**, 434 (1982).
[44] F. Lee, R. Kelly, L. Zhou, and W. Wilcox, Phys.Lett.

B627, 71 (2005), hep-lat/0509067.
[45] F. X. Lee, L. Zhou, W. Wilcox, and J. C. Christensen, Phys.Rev. **D73**, 034503 (2006), hep-lat/0509065.
[46] W. Detmold, B. Tiburzi, and A. Walker-Loud, Phys.Rev. **D73**, 114505 (2006), hep-lat/0603026.
[47] C. Aubin, K. Orginos, V. Pascalutsa, and M. Vanderhaeghen, Phys.Rev. **D79**, 051502 (2009), 0811.2440.
[48] W. Detmold, B. C. Tiburzi, and A. Walker-Loud, Phys.Rev. **D79**, 094505 (2009), 0904.1586.
[49] W. Detmold, B. Tiburzi, and A. Walker-Loud, Phys.Rev. **D81**, 054502 (2010), 1001.1131.
[50] T. Primer, W. Kamleh, D. Leinweber, and M. Burkardt, Phys.Rev. **D89**, 034508 (2014), 1307.1509.
[51] E. Luschevskaya, O. Teryaev, and O. Kochetkov (2014), 1411.4284.
[52] G. 't Hooft, Nucl.Phys. **B153**, 141 (1979).
[53] S. Beane et al. (NPLQCD), Phys.Rev. **D85**, 054511 (2012), 1109.2889.
[54] T. Yamazaki, K.-i. Ishikawa, Y. Kuramashi, and A. Ukawa, Phys.Rev. **D86**, 074514 (2012), 1207.4277.
[55] T. Yamazaki, K.-i. Ishikawa, Y. Kuramashi, and A. Ukawa (2015), 1502.04182.
[56] T. Yamazaki (2015), 1503.08671.
[57] M. Schindler and R. Springer, Prog.Part.Nucl.Phys. **72**, 1 (2013), 1305.4190.
[58] N. Barnea, L. Contessi, D. Gazit, F. Pederiva, and U. van Kolck, Phys.Rev.Lett. **114**, 052501 (2015), 1311.4966.
[59] R. G. Edwards and B. Joo (SciDAC Collaboration, LHPC Collaboration, UKQCD Collaboration), Nucl.Phys.Proc.Suppl. **140**, 832 (2005), hep-lat/0409003.